

You might find this additional information useful...

This article cites 35 articles, 15 of which you can access free at:

<http://ajpheart.physiology.org/cgi/content/full/274/5/H1705#BIBL>

This article has been cited by 20 other HighWire hosted articles, the first 5 are:

Nitrite reductase activity of hemoglobin as a systemic nitric oxide generator mechanism to detoxify plasma hemoglobin produced during hemolysis

P. C. Minneci, K. J. Deans, S. Shiva, H. Zhi, S. M. Banks, S. Kern, C. Natanson, S. B. Solomon and M. T. Gladwin

Am J Physiol Heart Circ Physiol, August 1, 2008; 295 (2): H743-H754.

[Abstract] [Full Text] [PDF]

Temporal and spatial variations of cell-free layer width in arterioles

S. Kim, R. L. Kong, A. S. Popel, M. Intaglietta and P. C. Johnson

Am J Physiol Heart Circ Physiol, September 1, 2007; 293 (3): H1526-H1535.

[Abstract] [Full Text] [PDF]

Transport and Peripheral Bioactivities of Nitrogen Oxides Carried by Red Blood Cell Hemoglobin: Role in Oxygen Delivery

P. Sonveaux, I. I. Lobysheva, O. Feron and T. J. McMahon

Physiology, April 1, 2007; 22 (2): 97-112.

[Abstract] [Full Text] [PDF]

Venular endothelium-derived NO can affect paired arteriole: a computational model

M. Kavdia and A. S. Popel

Am J Physiol Heart Circ Physiol, February 1, 2006; 290 (2): H716-H723.

[Abstract] [Full Text] [PDF]

Flash photolysis of caged nitric oxide inhibits proximal tubular fluid reabsorption in free-flow nephron

K.-P. Yip

Am J Physiol Regulatory Integrative Comp Physiol, August 1, 2005; 289 (2): R620-R626.

[Abstract] [Full Text] [PDF]

Medline items on this article's topics can be found at <http://highwire.stanford.edu/lists/artbytopic.dtl> on the following topics:

Biochemistry .. Guanylate Cyclase

Physiology .. Hemoglobins

Physiology .. Smooth Muscle

Neuroscience .. Nitric Oxide

Physiology .. Blood Circulation

Physiology .. Microcirculation

Updated information and services including high-resolution figures, can be found at:

<http://ajpheart.physiology.org/cgi/content/full/274/5/H1705>

Additional material and information about *AJP - Heart and Circulatory Physiology* can be found at:

<http://www.the-aps.org/publications/ajpheart>

This information is current as of July 5, 2009 .

Effective diffusion distance of nitric oxide in the microcirculation

MARK W. VAUGHN,¹ LIH KUO,² AND JAMES C. LIAO³

Departments of ¹Chemical Engineering and ²Medical Physiology, Texas A & M University, College Station, Texas 77843; and ³Department of Chemical Engineering, University of California, Los Angeles, California 90095-1592

Vaughn, Mark W., Lih Kuo, and James C. Liao. Effective diffusion distance of nitric oxide in the microcirculation. *Am. J. Physiol.* 274 (*Heart Circ. Physiol.* 43): H1705–H1714, 1998.—Despite its well-documented importance, the mechanism for nitric oxide (NO) transport in vivo is still unclear. In particular, the effect of hemoglobin-NO interaction and the range of NO action have not been characterized in the microcirculation, where blood flow is optimally regulated. Using a mathematical model and experimental data on NO production and degradation rates, we investigated factors that determine the effective diffusion distance of NO in the microcirculation. This distance is defined as the distance within which NO concentration is greater than the equilibrium dissociation constant (0.25 μM) of soluble guanylyl cyclase, the target enzyme for NO action. We found that the size of the vessel is an important factor in determining the effective diffusion distance of NO. In ~ 30 - to 100 - μm -ID microvessels the luminal NO concentrations and the abluminal effective diffusion distance are maximal. Furthermore, the model suggests that if the NO-erythrocyte reaction rate is as fast as the rate reported for the in vitro NO-hemoglobin reaction, the NO concentration in the vascular smooth muscle will be insufficient to stimulate smooth muscle guanylyl cyclase effectively. In addition, the existence of an erythrocyte-free layer near the vascular wall is important in determining the effective NO diffusion distance. These results suggest that 1) the range of NO action may exhibit significant spatial heterogeneity in vivo, depending on the size of the vessel and the local chemistry of NO degradation, 2) the NO binding/reaction constant with hemoglobin in the red blood cell may be much smaller than that with free hemoglobin, and 3) the microcirculation is the optimal site for NO to exert its regulatory function. Because NO exhibits vasodilatory function and antiatherogenic activity, the high NO concentration and its long effective range in the microcirculation may serve as intrinsic factors to prevent the development of systemic hypertension and atherosclerotic pathology in microvessels.

mathematical model; reaction kinetics; hemoglobin; endothelium; mass transport

ENDOTHELIAL RELEASE of nitric oxide (NO) has been documented to play an important role in the regulation of vascular tone and permeability (30), platelet adhesion and aggregation (36), smooth muscle proliferation (14), and endothelial cell-leukocyte interactions (18). NO in the microcirculation is of particular interest, since the majority of vascular resistance is found in <150 - μm -diameter microvessels. The transport of NO from the producing cell to the target cell is not well understood, since NO, as a free radical, can be degraded in a variety of reactions. It has been proposed that NO is transported from endothelial cells through diffusion and that cell membranes are readily permeable to NO

(28, 32). Under this hypothesis, NO diffuses from the endothelium into the surrounding smooth muscle or into the vascular lumen. The NO that diffuses into the vascular smooth muscle cells targets the enzyme guanylyl cyclase (32) to exert its vasoregulatory function. NO may also react with superoxide anion (31), bind with heme-containing proteins (5, 16), interact with enzymes containing iron-sulfur centers (30), or be degraded in several other reactions (1). Most importantly, NO reacts with deoxy- and oxyhemoglobin at a very high rate to form nitrosylhemoglobin [HbFe(II)NO] and methemoglobin [HbFe(III)] and nitrate, respectively. The bimolecular rate constants for these reactions are on the order of 25 – 50 $\mu\text{M}^{-1}\text{s}^{-1}$ (5, 9), which gives a half-life of 1 – 3 μs for NO under physiological conditions (hemoglobin concentration is ~ 2.3 mM in blood). If these reactions cause the concentration of NO to fall significantly below that needed to activate guanylyl cyclase, which has an equilibrium dissociation constant (k_{dis}) equal to 0.25 μM (41), then the biological function of NO will be diminished. Therefore, the effective diffusion distance of NO, which is defined as the distance within which NO concentration is greater than the k_{dis} of guanylyl cyclase, determines the functional range of NO action.

Several lines of in vivo and in vitro evidence suggest that hemoglobin is an effective NO scavenger that depletes NO. For example, injection of hemoglobin solution into experimental animals results in hypertension (15), most likely due to the oxidative reaction of NO with oxyhemoglobin in arterioles and surrounding tissue. Furthermore, 6 μM free hemoglobin can abolish NO-mediated vasodilation in vitro (7). These results suggest that the effect of hemoglobin on NO diffusion distance is significant. However, exactly how far NO diffuses away from the blood vessel and how hemoglobin affects diffusion distance remain unclear.

This NO reaction-diffusion problem was studied by Lancaster (21–23) using a modeling approach. He simplified the system by superimposing point sources of NO production and consumption. With his mathematical calculation, he concluded that NO could diffuse a relatively long distance from the source. This work (21), along with work reported by others (24, 43), represents the first generation of modeling effort on NO diffusion and reaction. However, three aspects need to be revised to examine the NO diffusion distance in the microcirculation. 1) The geometric factor was not considered. The source of NO production is, in fact, a surface source (proportional to vessel diameter), whereas NO consumption by hemoglobin in blood is a volumetric sink (proportional to the square of vessel

diameter). Therefore, the interaction between NO source and sink cannot be evaluated using the Lancaster model. 2) Superimposing point sources is a valid approximation of a surface source only if production and reaction follow the zeroth- or first-order kinetics with respect to NO. This approximation fails when the kinetic rate laws are nonlinear. 3) The parameters used previously (21–23) need to be reexamined for their effects on predicted NO concentration.

In this study we developed a mathematical formulation that is suitable for blood vessels and used mainly experimentally derived parameters to determine factors that affect the NO concentration and the effective diffusion distance, especially in the microcirculation. It should be emphasized that our goal is not to predict the actual concentration of NO in tissue. Rather, we are investigating the consequences of the diffusion-reaction hypothesis. Discrepancy between the model output and physiological data suggests possible points of deficiency of this proposed mechanism.

METHOD

Model assumptions. To model the NO concentration in blood vessels and parenchymal tissue, we divided this system into three compartments: the lumen, the endothelium, and the abluminal region (Fig. 1). The system was modeled using cylindrical coordinates. Because endothelial constitutive NO synthase is partially membrane bound, we considered NO to be produced from the luminal and abluminal sides of the endothelial cell membrane. These two sides of the endothelial cell were modeled as two singular surface sources, displaced by the average thickness of an endothelial cell. Furthermore, to make the system tractable, we made five assumptions. 1) The axial NO gradient along the vessel is small compared with the length of the region emitting NO, so NO transport by convection can be neglected. 2) We considered only the steady-state case in this study, although our model simulation also considers the time factor (see APPENDIX). 3) The rate of NO production from the endothelial cells does not vary with the vessel size. 4) Blood was treated as a continuum. In some cases, the particulate nature of blood was taken into account by recognizing the existence of a thin, erythrocyte-free layer near the vessel wall. This arrangement was modeled by including an erythrocyte-free region in the lumen. The thickness of this erythrocyte-free zone depends on fluid mechanical

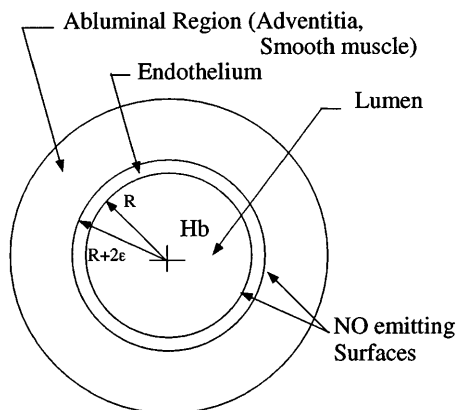


Fig. 1. Geometry of vessel, showing nitric oxide (NO)-producing surfaces of endothelium. r , Radial direction; R , inner radius; ϵ , half-thickness of endothelium.

considerations. 5) NO diffuses freely across cell membranes, and the diffusion coefficients for NO in all regions were taken to be the same. Because NO is dilute, the diffusion coefficient is assumed independent of concentration.

Model equations. With assumptions 1 and 2, the system can be treated as a one-dimensional problem, with NO concentration varying only in the radial direction (r). The balance between NO diffusion and reaction in all three compartments can be written for cylindrical coordinates as (see APPENDIX for detailed derivation)

$$D \frac{1}{r} \frac{d}{dr} r \frac{dc_{NO}}{dr} - V_{NO} = 0 \tag{1}$$

where c_{NO} is NO concentration, D is the diffusion coefficient, r is the radial distance from the vessel center, and V_{NO} is the lumped reaction rate at which NO is consumed by various chemical reactions. Equation 1 is used for all three regions of the vessel, although the rate expression for V_{NO} may differ in each region. In the endothelium and the abluminal region, it takes the following form

$$V_{NO} = k_{n,ab} c_{NO}^n \tag{2}$$

where $k_{n,ab}$ is the reaction rate constant and the order of the reaction (n) was taken to be 2. In the luminal region, NO consumption by hemoglobin in the bloodstream can be expressed by the rate equation

$$V_{NO} = k_{2,lu} c_{NO} c_{Hb} \tag{3}$$

$$\approx k_{1,lu} c_{NO} \tag{4}$$

where $k_{2,lu}$ and $k_{1,lu}$ are the rate constants and c_{Hb} is the hemoglobin concentration in the lumen. In Eqs. 3 and 4 we have recognized that c_{Hb} is essentially constant, so the reaction can be considered pseudo-first order in NO with the rate constant $k_{1,lu} = k_{2,lu} c_{Hb}$.

Boundary conditions. In this system, NO is produced from two concentric surfaces separated by a distance of 2.5 μm , the approximate thickness of the endothelial cell (19). For a vessel of inner radius R , the boundary conditions at the lumen-endothelium interface ($r = R$) are given by (see APPENDIX)

$$D \left. \frac{dc_{NO}}{dr} \right|_{lu} - D \left. \frac{dc_{NO}}{dr} \right|_{ec} = \dot{q}_{NO,lu} \tag{5}$$

$$c_{NO|lu} = c_{NO|ec} \tag{6}$$

and at the endothelium-abluminal region interface, $r = R + 2\epsilon$

$$D \left. \frac{dc_{NO}}{dr} \right|_{ec} - D \left. \frac{dc_{NO}}{dr} \right|_{ab} = \dot{q}_{NO,ab} \tag{7}$$

$$c_{NO|ec} = c_{NO|ab} \tag{8}$$

The subscripts lu, ec, and ab specify that the quantities are evaluated in the lumen, the endothelial cell, and the abluminal parenchyma, respectively. Note that the quantity $D dc_{NO}/dr$ was evaluated at each region and, in general, will be different on each side of the interface as the NO-producing boundary is approached. The total NO production rate per unit area of the endothelium is $\dot{q}_{NO} = \dot{q}_{NO,lu} + \dot{q}_{NO,ab}$, where $\dot{q}_{NO,lu}$ and $\dot{q}_{NO,ab}$ are the NO production rates from the luminal and abluminal sides of the endothelial membrane, respectively. From the data of Malinski et al. (28), we assume that $\dot{q}_{NO,lu} = \dot{q}_{NO,ab}$. Another boundary condition is implied by the symmetry of

the vessel

$$\frac{dc_{\text{NO}}}{dr} = 0 \quad \text{at } r = 0 \quad (9)$$

and finally, far from the vessel we have

$$\frac{dc_{\text{NO}}}{dr} = 0 \quad \text{at } r \rightarrow \infty \quad (10)$$

These six boundary conditions (Eqs. 5–10), together with the governing equations for the three regions, can be solved for NO concentration at steady state as a function of r .

Model parameters. The parameters in the model include the diffusion coefficient of NO (D), the NO production rate (\dot{q}_{NO}), and the rate constant of NO degradation in each region. The diffusion coefficient of NO has been determined to be between 3,300 and 4,500 $\mu\text{m}^2 \cdot \text{s}^{-1}$. We used 3,300 $\mu\text{m}^2 \cdot \text{s}^{-1}$, which is consistent with our estimate from the data of Malinski et al. (28) and close to the diffusion coefficient of O_2 , i.e., 1,300–2,000 $\mu\text{m}^2 \cdot \text{s}^{-1}$ (12). According to *assumption 5*, the NO diffusion coefficients in all the regions are assumed to be the same.

The rate of NO production by the endothelium surfaces and the NO consumption rate constant in the endothelium and the abluminal region were estimated by fitting the data of Malinski et al. (28) to a similar model based on oblate spherical coordinates (42). The \dot{q}_{NO} was estimated to be $5.3 \times 10^{-14} \mu\text{mol} \cdot \mu\text{m}^{-2} \cdot \text{s}^{-1}$. The second-order rate law for NO consumption provided the best fit to the data, but the difference between the first- and second-order rate law was insufficient to exclude the first-order rate law. The reaction rate coefficient ($k_{2,\text{ab}}$) was estimated to be $0.05 \mu\text{M}^{-1} \cdot \text{s}^{-1}$ if V_{NO} is assumed to be second order. These computations have been detailed elsewhere (42).

The rate constant for NO consumption by hemoglobin in the lumen ($k_{1,\text{lu}}$, according to Eq. 4) was initially taken to be $2.3 \times 10^5 \text{ s}^{-1}$, which was calculated from the in vitro rate constant between NO and free hemoglobin (6, 9), with the assumption that the hemoglobin concentration in blood is 2.3 mM (tetramer). Because of uncertainty, several values for $k_{1,\text{lu}}$ were used for the computations that follow. These range from 2.3×10^5 to 15 s^{-1} . The solution of the model equations is discussed in the APPENDIX.

RESULTS

Hemoglobin is an effective NO scavenger. The above model was used to calculate the NO concentration in the vascular lumen and the abluminal region of an NO-producing vessel with a diameter of 100 μm . In this case, the second-order reaction rate law was used to describe NO consumption in the endothelium and the abluminal region, and no erythrocyte-free zone was considered. To examine the significance of NO reaction with hemoglobin, we used a wide range of rate constants, $k_{1,\text{lu}}$, in the calculation. Figure 2 shows the NO concentration in the vicinity of the vessel. When the reaction rate in the lumen is high (large $k_{1,\text{lu}}$), the blood acts as a sink for NO. For example, when $k_{1,\text{lu}} = 2.3 \times 10^5 \text{ s}^{-1}$, >99% of the NO produced flows into the lumen and <1% is available to diffuse into the vascular smooth muscle (results not shown). If this rate constant is estimated on the basis of the in vitro hemoglobin-NO reaction, $k_{1,\text{lu}} = 2.3 \times 10^5 \text{ s}^{-1}$ (6, 9), the NO concentrations in all the regions are much less than the k_{dis} of

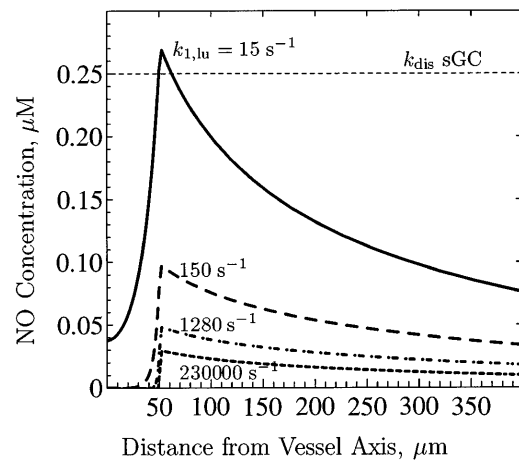


Fig. 2. NO concentration in blood and abluminal region depends on NO reaction rate in blood. This dependence is shown for a 100- μm -diameter vessel, with NO production rate (\dot{q}_{NO}) = $5.3 \times 10^{-14} \mu\text{mol} \cdot \mu\text{m}^{-2} \cdot \text{s}^{-1}$ and abluminal rate constant ($k_{2,\text{ab}}$) = $0.05 \mu\text{M}^{-1} \cdot \text{s}^{-1}$. Rate coefficient for NO reaction in blood ($k_{1,\text{lu}}$) = $2.3 \times 10^5 \text{ s}^{-1}$ estimated for free Hb at concentration of whole blood (6, 9) (dotted line), $k_{1,\text{lu}} = 1,280 \text{ s}^{-1}$ estimated from deoxygenated erythrocytes (5) (dashed-dotted line), $k_{1,\text{lu}} = 150 \text{ s}^{-1}$ estimated from Hb concentration found to abolish NO effects (34) (dashed line), and $k_{1,\text{lu}} = 15 \text{ s}^{-1}$ estimated by fitting model to NO concentration measurements on human blood (40) (solid line). Only last case gives NO concentration exceeding k_{dis} of guanylyl cyclase (sGC).

soluble guanylyl cyclase. Under this condition, NO cannot effectively stimulate guanylyl cyclase.

Because of the uncertainty of the NO-blood reaction rate, we considered other estimates of $k_{1,\text{lu}}$. If the NO-deoxy erythrocyte reaction rate from Carlsen and Comroe (5) was used to estimate $k_{1,\text{lu}}$, 1,280 s^{-1} was obtained. However, this value still gives an NO concentration much lower than the k_{dis} of soluble guanylyl cyclase (Fig. 2). For NO concentration in the vascular smooth muscle to reach k_{dis} , $k_{1,\text{lu}}$ has to be $<15 \text{ s}^{-1}$. If $k_{1,\text{lu}}$ exceeds $\sim 15 \text{ s}^{-1}$, the NO concentration would not reach the k_{dis} of guanylyl cyclase, and thus the effective diffusion distance is zero. In these cases, the local NO concentration is not sufficient to activate guanylyl cyclase in the vascular smooth muscle cells. Therefore, these calculations provide boundaries for the effective NO-erythrocyte reaction rate constant under the free diffusion hypothesis.

Erythrocyte-free layer increases the mass transfer resistance. In the above calculation, the blood is assumed to be a continuum. It can be argued, however, that if the particulate nature of the blood is taken into consideration, the erythrocyte-free layer near the vascular wall may provide sufficient mass transfer resistance to reduce the NO-scavenging effect of the blood. To analyze this situation, an erythrocyte-free region adjacent to the luminal side of the endothelium is included in the model. In this region, NO is not consumed by hemoglobin in blood. Rather, it is likely to be consumed by O_2 in plasma with a rate law second order in NO and first order in O_2 . With a dissolved O_2 concentration in plasma of $\sim 27 \mu\text{M}$ (35), the rate constant, $k_{2,\text{ef}}$, where the subscript indicates the erythrocyte-free region, is estimated to be $0.002 \mu\text{M}^{-1} \cdot \text{s}^{-1}$. The thickness of the

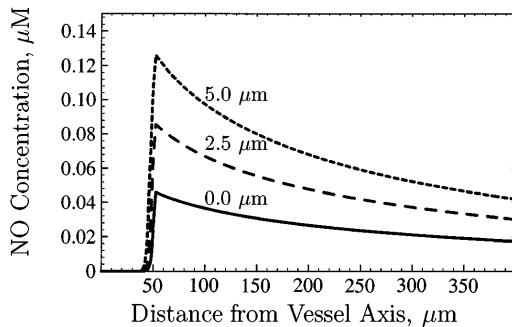


Fig. 3. Effect of erythrocyte-free layer on NO concentration profiles for 100- μm -diameter blood vessel. Parameters are as follows: $k_{1,\text{lu}} = 1,280 \text{ s}^{-1}$, $\dot{q}_{\text{NO}} = 5.3 \times 10^{-14} \mu\text{mol} \cdot \mu\text{m}^{-2} \cdot \text{s}^{-1}$, and $k_{2,\text{ab}} = 0.05 \mu\text{M}^{-1} \cdot \text{s}^{-1}$. Numbers on curves (0.0, 2.5, and 5.0 μm) indicate thickness of erythrocyte-free layer.

erythrocyte-free zone (δ) depends on fluid mechanical considerations; we expected $\delta = 2.5 \mu\text{m}$ (38) for a 100- μm -diameter vessel. The NO consumption rate constant ($k_{1,\text{lu}}$) in the erythrocyte-rich lumen is taken to be $1,280 \text{ s}^{-1}$ as an illustration. Other parameters were the same as the above case. Figure 3 shows that under these conditions the endothelial and abluminal NO concentration increased almost twofold for $\delta = 2.5 \mu\text{m}$. However, the abluminal NO concentration still falls below the k_{dis} of guanylyl cyclase. Therefore, the existence of the erythrocyte-free layer cannot prevent the NO-scavenging effect if the NO-hemoglobin reaction is already very fast. The impact of the erythrocyte-free layer on the NO diffusion distance is diminished when $k_{1,\text{lu}}$ decreased (results not shown).

NO effective diffusion distance depends on the vessel diameter. Because the vascular properties such as the sensitivities to adenosine, shear stress, and transmural pressure exhibit significant variation with vessel diameter (20), we investigated effective diffusion distance for NO in microvessels of various sizes. Although the NO production rate per endothelial cell (or per unit surface area of the endothelium) is assumed to be constant regardless of vessel size, larger vessels have a lower surface-to-volume ratio, which may affect the NO diffusion distance. Moreover, smaller vessels are known to have a lower hematocrit (7), which reduces the NO consumption rate in the lumen. To investigate the effect of these factors, we considered three cases. The first simulates the condition where physiological solution is perfused. In this case, the NO-hemoglobin reaction is absent in the lumen, and NO degradation in this region is assumed to be second order, with $k_{2,\text{lu}} = 0.002 \mu\text{M}^{-1} \cdot \text{s}^{-1}$. Other parameters are as indicated in the legend of Figure 4. The effective diffusion distance was calculated as a function of vessel diameter. As shown in Fig. 4A, the effective diffusion distance increases as diameter increases. This result is due to the geometry of the vessel: as vessel size increases, the total endothelial production of NO increases, which drives the NO diffusion further.

When blood is perfused in the vessels, the results are different. In the second case, we considered the situation where blood with constant hematocrit is perfused

through vessels of different sizes. No erythrocyte-free layer was considered here for simplicity. The luminal NO consumption rate constant, $k_{1,\text{lu}}$, was taken to be 15 s^{-1} , since higher values give zero effective diffusion distance. Interestingly, the effective diffusion distance exhibits a maximum as vessel diameter increases (Fig. 4A). The optimal vessel size for NO diffusion is 30–100 μm in diameter. This phenomenon is attributed to the combined effect of NO production from the endothelium and NO scavenging by the blood. The total NO production increases linearly with the vessel diameter, whereas the luminal blood volume increases with the square of the vessel diameter.

In vivo, because of the Fåhræus effect, the hematocrit decreases as vessel diameter decreases (7). In the third case, we took this phenomenon into account using literature data for the correlation between hematocrit and vessel diameter (7). The change in hematocrit is reflected in $k_{1,\text{lu}}$, which is proportional to the total hemoglobin concentration in the vascular lumen. Figure 4A shows that the peak of the effective NO diffusion distance is even more pronounced here than for the second case. The location of the peak in the blood-perfused cases suggests that the most effective region for NO to exert its function is in $\sim 20\text{-}\mu\text{m}$ -diameter arterioles. The effective diffusion distance is sharply decreased in $<20\text{-}\mu\text{m}$ -diameter vessels. For small and large arteries ($>200 \mu\text{m}$), the effective NO diffusion distance may be less than the thickness of the smooth

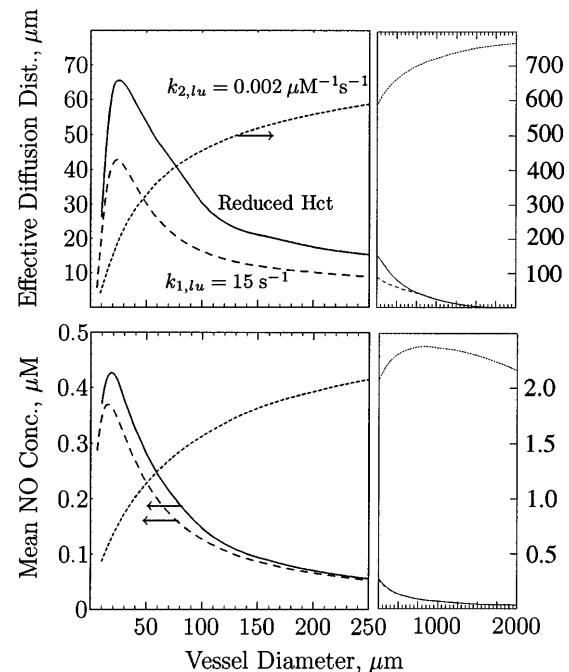


Fig. 4. *A*: effective diffusion distance as a function of vessel diameter for vessels perfused with O_2 -saturated physiological salt solution ($k_{2,\text{lu}} = 0.002 \mu\text{M}^{-1} \cdot \text{s}^{-1}$, dotted line), vascular network perfused with blood with assumption of constant hematocrit (Hct; $k_{1,\text{lu}} = 15 \text{ s}^{-1}$, dashed line), and vascular network perfused with blood with Hct variation taken into account [$k_{1,\text{lu}} = 10 \text{ s}^{-1}$ for a 24- μm -diameter vessel to 15 s^{-1} for a 2,000- μm -diameter vessel (solid line)]. *B*: mean plasma concentration of NO under conditions in *A*. For both plots, $k_{2,\text{ab}} = 0.05 \mu\text{M}^{-1} \cdot \text{s}^{-1}$ and $\dot{q}_{\text{NO}} = 5.3 \times 10^{-14} \mu\text{mol} \cdot \mu\text{m}^{-2} \cdot \text{s}^{-1}$.

muscle layer. These results indicate that the arterioles, 20–100 μm in diameter, may be a primary action site for NO to exert its biological function in terms of regulating downstream pressure and perfusion.

The mean luminal NO concentrations for the above three cases as a function of vessel diameter are shown in Fig. 4B. The diameter dependence of the mean luminal NO concentration closely resembles that of the effective diffusion distance, although the effect of varying the hematocrit is much less pronounced. For larger vessels, the mean NO concentration does not depend strongly on vessel size. These results indicate that NO concentration and effective diffusion distance may exhibit spatial heterogeneity in a vascular network.

DISCUSSION

In the blood vessels the luminal release of NO from the endothelium has been shown to prevent platelet aggregation and to inhibit the adhesion of platelets, neutrophils, and lymphocytes to the endothelial surface (18, 36). The abluminal presence of NO inhibits smooth muscle contraction, proliferation, and migration (14, 30). Although the physiological and pathophysiological significance of NO has been well documented, the problem of NO transport has been unresolved.

In addition to the free diffusion hypothesis (28, 32) described above, a nitrosyl thiol-mediated transport hypothesis (17) has been proposed. However, none of these hypotheses accounted for all the details of the NO transport in vivo. In particular, the role of hemoglobin as an NO scavenger and the effect of vessel diameter deserve further attention. We have explored the free diffusion hypothesis by synthesizing the diffusion and reaction processes of NO into a mathematical model with experimentally derived parameters.

NO-hemoglobin reaction rate. Because of the uncertainty of the NO-hemoglobin reaction rate in vivo, we examined a wide range of rate constants for this reaction (Fig. 2). The highest $k_{1,\text{lu}}$ ($2.3 \times 10^5 \text{ s}^{-1}$) corresponds to the in vitro NO-hemoglobin reaction rate constant (6, 9) combined with the average physiological hemoglobin concentration in the whole blood (2.3 mM tetramer). The in vitro NO-hemoglobin reaction is first order in hemoglobin and NO, with a second-order rate constant of $25 \mu\text{M}^{-1} \cdot \text{s}^{-1}$ (5, 6). This rate constant, although evaluated for free deoxyhemoglobin, is similar to that for free oxyhemoglobin (9). Figure 2 shows that, with this $k_{1,\text{lu}}$, the NO concentration in the abluminal region is significantly below the k_{dis} of guanylyl cyclase.

For hemoglobin in deoxy erythrocytes, the NO-erythrocyte reaction rate constant, measured to be $0.14 \mu\text{M}^{-1} \cdot \text{s}^{-1}$ [the mean of the data of Carlsen and Comroe (5)], and an average hemoglobin concentration (2.3 mM) result in $k_{1,\text{lu}} = 1,280 \text{ s}^{-1}$. Figure 2 shows that this rate constant still leads to an NO concentration much lower than that necessary for activating guanylyl cyclase.

Another estimate for $k_{1,\text{lu}}$ may be obtained from the minimum free hemoglobin concentration that causes significantly increased vascular resistance, since the

value of $k_{1,\text{lu}}$ for blood must be less than this value. For perfused rabbit hearts, Pohl and Lamontagne (34) reported this level to be 6 μM free hemoglobin. The $k_{1,\text{lu}}$ corresponding to this hemoglobin concentration is 150 s^{-1} (half time = 0.005 s). As expected, this value gives an NO concentration lower than the k_{dis} of guanylyl cyclase (Fig. 2).

Finally, we determined the $k_{1,\text{lu}}$ that gives a mean free NO concentration in the blood corresponding to that measured experimentally: 0.0034 μM (40). If the blood was taken from a 4-mm-diameter vessel and if the effect of the erythrocyte-free layer is ignored, this corresponds to $k_{1,\text{lu}} = 15 \text{ s}^{-1}$ (half-time = 0.05 s) according to our model. Now, this value gives an abluminal NO concentration that is sufficient to activate guanylyl cyclase (Fig. 2). Although the estimation of this value is crude, it provides the order of magnitude of the reaction rate constant that gives an NO concentration exceeding the k_{dis} of guanylyl cyclase.

One possible explanation for the low NO concentration predicted from the in vitro NO-free hemoglobin reaction rate constant is that the erythrocyte-free layer near the blood vessel may provide a mass transfer barrier to slow the NO-erythrocyte reaction. For a flowing suspension, such as blood, the time-averaged concentration of cells varies with position. Because of hydrodynamic interactions, cells migrate toward the center of the vessel, leaving a thin layer of fluid near the vessel wall in which there are few cells (38). We approximate this distribution by a uniform concentration in the interior of the vessel and a 2.5- μm -thick erythrocyte-free layer adjacent to the endothelium. This layer introduces mass transfer resistance, which diminishes the effective reaction rate in the lumen of the vessel. In Fig. 3 we see that the erythrocyte-free layer does raise the NO concentration appreciably. However, it cannot account for the difference between the NO concentration measured in vivo and the NO concentration predicted from the in vitro NO-hemoglobin reaction rate. This and the previous results (Fig. 2) suggest that the NO-erythrocyte reaction in vivo is much slower than the NO-hemoglobin reaction in vitro or that the NO is transported by other mechanisms not accounted for in the model.

Free hemoglobin has been proposed to be used as a blood substitute. However, because of the NO-hemoglobin interaction, the administration of free hemoglobin causes vasoconstriction and possibly hypertension (44). Site-directed mutagenesis has been used to create mutant hemoglobins that have reduced the NO-hemoglobin interaction by 37-fold (9). Our model suggests that reduction of the NO-hemoglobin interaction may be achieved by enclosing hemoglobin in erythrocytes. Thus free hemoglobin-induced hypertension may be mitigated by packaging hemoglobin for blood substitutes in a cell-like manner.

Vessel diameter dependency of the effective NO diffusion distance. Among the findings, the effect of vessel size on the luminal NO concentration and the effective NO diffusion distance in the abluminal region are the most unexpected (Fig. 4). The model suggests that in

the domain of the microcirculation an optimal range of vessel diameters exists, within which the effective NO diffusion distance is maximized. This conclusion is predicated on the free diffusion-reaction mechanism of NO. On the basis of this mechanism, we examine the possible implications of this conclusion and discuss possible experimental supports.

The wall thickness of 10- to 100- μm -ID microvessels is $\sim 5\text{--}8\ \mu\text{m}$ (Ref. 2; L. Kuo, unpublished observations in isolated and pressurized coronary arterioles), which is less than the effective diffusion distance. However, for $>400\text{-}\mu\text{m}$ -diameter vessels, the effective NO diffusion distance may not cover the whole thickness of the vascular smooth muscle layer (Fig. 4A), and thus the vasodilation property of NO may be compromised. Indeed, $>200\text{-}\mu\text{m}$ -diameter vessels show little NO-mediated vasodilation in response to increased shear stress (20). The existence of an optimal vessel diameter for NO diffusion is a result of the competition between increased NO production surface and increased NO-scavenging blood volume in the lumen as the diameter increases. The effective diffusion distance can be enhanced by the reduction of hematocrit in microvessels in vivo. It is worth noting that luminal and perivascular PO_2 in microcirculation decreases as vessel size decreases (8, 33). The reduction in PO_2 is likely to reduce the NO degradation rate in the blood and in the abluminal region and thus increases the effective diffusion distance of NO. This phenomenon may enhance the diameter dependency of the effective NO diffusion distance in the microcirculation.

Our model also suggests that the microvessels are most sensitive to shear stress, provided that a given shear stress induces equal NO production per endothelial cell in vessels of different sizes. This is seen from the effective diffusion distance in Fig. 4A, which was calculated with a constant NO production rate. If the NO production rate decreases, e.g., by reducing shear stress, the curves in Fig. 4A will move down almost proportionally. For example, if the NO production is stimulated to 50% of the value used in Fig. 4A, the effective NO diffusion distance (the solid line in Fig. 4A) can cover only the smooth muscle layers of $\sim 30\text{-}$ to $100\text{-}\mu\text{m}$ -diameter vessels. The effective NO diffusion distance in vessels outside this diameter range will not cover the whole smooth muscle layer, and thus these vessels will not be sufficiently dilated by NO. Consequently, on the basis of the model calculation, 30- to $100\text{-}\mu\text{m}$ -ID vessels will have a lower threshold for shear-induced dilation than smaller or larger vessels. This prediction is qualitatively supported by experimental results (20) which show that 60- to $100\text{-}\mu\text{m}$ -ID vessels, in comparison to their downstream and upstream vessels, exhibit the lowest threshold for shear-induced dilation.

The diameter dependency of NO diffusion suggests that the microcirculation is optimally situated for NO to exert its regulatory function. Microvessels with different sizes have been shown to exhibit different regulatory properties (20), which may reflect the longitudinal integration of regulatory mechanism (25). Small

arterioles (40–90 μm) and venules that are arranged in parallel may communicate and interact (11, 37), contributing to the integrated control of the microcirculation. It has been shown that NO-mediated, shear-induced dilation in intermediate and large arterioles is particularly important for flow regulation (25). It appears that the circulation system takes full advantage of the size dependency of NO diffusion distance and builds the control mechanism accordingly.

Because our model predicts that 30- to $100\text{-}\mu\text{m}$ -diameter microvessels exhibit the optimal NO efficiency, it is expected that inhibition of NO synthesis would produce a significant constriction of these vessels. Indeed, this view is supported by an in vivo study of skeletal muscle microcirculation showing that inhibition of NO synthesis predominantly increases vascular resistance in $>25\text{-}\mu\text{m}$ -diameter microvessels (10). Moreover, because the antiatherogenic property of NO has been demonstrated (27, 39), vessel size dependence of NO concentration may be one of the factors responsible for the difference in the vascular pathology between large vessels and microvessels during the development of atherosclerosis. For example, microvessels do not develop atherosclerotic lesions (29), possibly because of the higher NO concentration in these vessels.

Modeling studies. Although previous workers have made important contributions to the analysis of NO diffusion (21–24, 28, 43), this problem deserves further investigation. The approach outlined here considers the geometry of NO production and consumption regions and provides a more general analysis of NO reaction and diffusion. Although we considered only the steady-state behavior of the system, the numerical simulation did take into account the transient behavior, as discussed in the APPENDIX. More regions can be added to the model, if desired. For example, myoglobin-containing cells in muscle are expected to consume NO at a much higher rate than others. The model can be extended to account for this effect by considering a myoglobin-containing region. Our analysis here highlights the importance of analyzing diffusion and reaction quantitatively, which echoes the theme emphasized by many previous workers (3, 4, 13, 23, 26, 33).

APPENDIX

Governing Equations

General form. Here the general form of the governing equations is stated. The concentration of a diffusing, reacting substance, such as NO, is described by the species mass balance (4A). For NO, this balance can be written as

$$\frac{\partial c_{\text{NO}}}{\partial t} = D\nabla^2 c_{\text{NO}} - \nabla c_{\text{NO}} \cdot \mathbf{v} - V_{\text{NO}} \quad (A1)$$

where ∇ is the vector gradient operator, ∇^2 is the Laplacian operator, c_{NO} is the concentration of NO, and V_{NO} is the rate at which NO is consumed by reaction. Two processes are involved in the transfer of NO: the first term on the right-hand side represents the diffusion of NO; the second represents the transport of NO by a molar averaged velocity \mathbf{v} .

Cylindrical coordinates. For a trace component diffusing into a one-dimensional cylindrical flow with no axial concen-

tration gradients, $\nabla_{\text{cNO}} \cdot \mathbf{v} = 0$, since only v_z and dc_{NO}/dr are nonzero. For first-order NO consumption under steady-state conditions, $\partial c_{\text{NO}}/\partial t = 0$ and $V_{\text{NO}} = k_{1,\text{NO}}c_{\text{NO}}$. With these simplifications the dimensionless form of Eq. A1 becomes

$$\frac{1}{r^*} \frac{d}{dr^*} \left(r^* \frac{dc_{\text{NO}}^*}{dr^*} \right) - k^* c_{\text{NO}}^* = 0 \quad (\text{A2})$$

The dimensionless distance (r^*), the dimensionless concentration (c_{NO}^*), and the dimensionless reaction rate coefficient (k^* , the Damköhler number) are defined by

$$r = \frac{r}{r_0}, \quad c_{\text{NO}}^* = \frac{c_{\text{NO}}}{c_0}, \quad k^* = \frac{r_0^2 k_{1,\text{NO}}}{D} \quad (\text{A3})$$

Here, the characteristic length (r_0) is the vessel radius, and the characteristic concentration (c_0) is taken to be 1 μM , the order of the magnitude of the steady-state concentration measured by Malinski et al. (2A). Equation A2 shows that for a first-order reaction the steady-state concentration profile depends only on k^* . Thus, for a given vessel size, the concentration profile is fixed by the ratio of reaction constant to diffusion constant.

For an n th-order reaction, $V_{\text{NO}} = k_{1,\text{NO}}c_{\text{NO}}^n$, we have a similar situation

$$\frac{1}{r^*} \frac{d}{dr^*} \left(r^* \frac{dc_{\text{NO}}^*}{dr^*} \right) - k_n^* (c_{\text{NO}}^*)^n = 0 \quad (\text{A4})$$

and

$$k_n^* = \frac{r_0^2 c_0^{(n-1)} k_{n,\text{NO}}}{D} \quad (\text{A5})$$

Boundary conditions. The NO distribution in each of the three regions, the lumen, the endothelium, and the abluminal region, is governed by Eq. A1 with the regions linked by conditions at their boundaries. Six boundary conditions and three initial conditions are needed to solve the complete time-varying problem. Here we are interested in the steady-state case, Eq. A2, which requires only the six boundary conditions and no initial conditions.

Production and mass transfer of a substance from the singular surfaces bounding the endothelium are described by the surface mass balance (sometimes called the jump mass balance) (4A). Because the NO consumption in the luminal region is different from that in the abluminal region (and possibly, the endothelial cell itself), the NO gradient and the flux of NO in each of the regions will also differ. The jump mass balance related the fluxes to the production rate. For NO produced at the interface between regions 1 and 2, this balance can be written as

$$c_{\text{NO}}(\mathbf{v}_{\text{NO}} - \mathbf{u})|_1 \cdot \mathbf{n}_1 - c_{\text{NO}}(\mathbf{v}_{\text{NO}} - \mathbf{u})|_2 \cdot \mathbf{n}_1 = \dot{q}_{\text{NO}} \quad (\text{A6})$$

where \mathbf{n}_1 is the normal vector pointing to region 1. The NO concentration is denoted c_{NO} , \mathbf{v}_{NO} is the molar average velocity of NO at the interface, \mathbf{u} is the velocity of the interface, and \dot{q}_{NO} is the rate at which NO is produced by a unit of surface area ($\text{mol} \cdot \text{time}^{-1} \cdot \text{area}^{-1}$). The notation $|_i$ means that the concentration and velocities are evaluated in phase i , as the interface is approached. Equation A6 related the velocity of NO at an interface to the velocity of the interface and the production rate of NO. At steady state the vessel diameter no longer changes with time, so $\mathbf{u} = 0$.

The product $c_{\text{NO}}\mathbf{v}_{\text{NO}} \equiv \mathbf{N}$ (mass transported per unit time per unit area) is denoted the mass flux vector. For a trace

quantity like NO, it can be expressed in the form of Fick's law

$$\mathbf{N} = c_{\text{NO}}\mathbf{v} - D\nabla c_{\text{NO}} \quad (\text{A7})$$

where \mathbf{v} is the total molar average velocity. The first term on the right-hand side represents the transport of NO by an overall molar average velocity; the second represents the diffusion of NO. For a trace quantity diffusing from a surface that is essentially impermeable to fluid, $\mathbf{v} = 0$ at the surface. In view of this, the boundary condition at each endothelial surface can be obtained by combining Eqs. A6 and A7

$$\dot{q}_{\text{NO}} = \mathbf{N}_1 \cdot \mathbf{n}_1 - \mathbf{N}_2 \cdot \mathbf{n}_1 \quad (\text{A8a})$$

$$= D_1 \nabla c_{\text{NO}}|_1 \cdot \mathbf{n}_1 - D_2 \nabla c_{\text{NO}}|_2 \cdot \mathbf{n}_1 \quad (\text{A8b})$$

where $|_i$ means that the diffusion coefficient and concentration gradient are evaluated in region i . Equation A8 is valid for any coordinate system.

At the endothelium-lumen interface of a cylindrical vessel, Eq. A8 reduces to

$$\begin{aligned} \dot{q}_{\text{NO,lu}}(t) &= \mathbf{N}_{\text{lu}} \cdot \mathbf{n}_{\text{lu}} - \mathbf{N}_{\text{ec}} \cdot \mathbf{n}_{\text{lu}} \\ &= D_{\text{lu}} \left. \frac{dc_{\text{NO}}}{dr} \right|_{\text{lu}} - D_{\text{ec}} \left. \frac{dc_{\text{NO}}}{dr} \right|_{\text{ec}} \end{aligned} \quad (\text{A9})$$

At the endothelium-abluminal region interface, Eq. A8 reduces to

$$\begin{aligned} \dot{q}_{\text{NO,ab}}(t) &= \mathbf{N}_{\text{ec}} \cdot \mathbf{n}_{\text{ab}} - \mathbf{N}_{\text{ab}} \cdot \mathbf{n}_{\text{ab}} \\ &= D_{\text{ec}} \left. \frac{dc_{\text{NO}}}{dr} \right|_{\text{ec}} - D_{\text{ab}} \left. \frac{dc_{\text{NO}}}{dr} \right|_{\text{ab}} \end{aligned} \quad (\text{A10})$$

where \mathbf{N}_{lu} is the flux of NO from the producing surface into the lumen, \mathbf{N}_{ab} is the flux of NO at the producing surface into the abluminal region, \mathbf{N}_{ec} is the flux of NO at the producing surface into the endothelial section, \mathbf{n}_{lu} is the unit normal vector pointing in the lumen, \mathbf{n}_{ab} is the unit normal vector pointing into the abluminal region, and $\dot{q}_{\text{NO}}(t) = \dot{q}_{\text{NO,lu}}(t) + \dot{q}_{\text{NO,ab}}(t)$ is the total NO production rate per unit area of endothelium, which was estimated from the data of Malinski et al. (2A). Without evidence to the contrary, we assume $\dot{q}_{\text{NO,lu}}(t) = \dot{q}_{\text{NO,ab}}(t)$.

At these interfaces, continuity of NO concentrations supplies another two boundary conditions

$$c_{\text{NO}}|_{\text{lu}} = c_{\text{NO}}|_{\text{ec}} \quad (\text{A11a})$$

at the luminal-endothelium interface

$$c_{\text{NO}}|_{\text{ec}} = c_{\text{NO}}|_{\text{ab}} \quad (\text{A11b})$$

at the endothelium-abluminal interface

It would be better to require the partial pressure of NO to be continuous rather than the concentration. However, there are few data for NO solution properties, particularly in tissue, so we assume continuity of concentration as a first approximation.

When the NO production from the endothelium is uniform around the vessel, as we have stated in assumption 1, the concentration in the vessel is symmetrical about the axis

$$\left. \frac{dc_{\text{NO}}}{dr} \right|_{r=0} = 0, \quad \text{at } r = 0 \quad (\text{A12})$$

Other boundary conditions can be fixed far from the produc-

ing surface where the NO concentration changes slowly; therefore

$$\frac{dc_{\text{NO}}}{dr} = 0, \quad \text{far from the endothelium, } r \rightarrow \infty \quad (A13)$$

In dimensionless form the boundary conditions at the endothelium (Eqs. A9–A11) take the form

$$c_{\text{NO}}^*|_{\text{lu}} = c_{\text{NO}}^*|_{\text{ec}} \quad (A14a)$$

$$\dot{q}_{\text{NO,lu}}^* = D_{\text{lu}}^* \left. \frac{dc_{\text{NO}}^*}{dr^*} \right|_{\text{lu}} - \left. \frac{dc_{\text{NO}}^*}{dr^*} \right|_{\text{ec}} \quad (A14b)$$

$$c_{\text{NO}}^*|_{\text{ec}} = c_{\text{NO}}^*|_{\text{ab}} \quad (A15a)$$

$$\dot{q}_{\text{NO,ab}}^* = \left. \frac{dc_{\text{NO}}^*}{dr^*} \right|_{\text{ec}} - D_{\text{ab}}^* \left. \frac{dc_{\text{NO}}^*}{dr^*} \right|_{\text{ab}} \quad (A15b)$$

where we have defined dimensionless production and dimensionless diffusion coefficient

$$\dot{q}_{\text{NO,lu}}^* = \frac{r_0 \dot{q}_{\text{NO,lu}}}{c_0 D_{\text{ec}}}, \quad D_{\text{lu}}^* = \frac{D_{\text{lu}}}{D_{\text{ec}}}, \quad (A16)$$

$$\dot{q}_{\text{NO,ab}}^* = \frac{r_0 \dot{q}_{\text{NO,ab}}}{c_0 D_{\text{ec}}}, \quad D_{\text{ab}}^* = \frac{D_{\text{ab}}}{D_{\text{ec}}}$$

Comparing Eqs. A2 and A3 with Eqs. A14b and A15b, we can make an interesting observation. The diffusion coefficient appears in the mass balance Eq. A2 coupled with the reaction coefficient, so a smaller diffusion coefficient has the same effect as a larger reaction coefficient: it makes the concentration fall off more rapidly with distance. The effect of diffusion coefficient is different at the boundary. Here a smaller diffusion coefficient has the same effect as increasing the production rate: it increases the NO concentration in the neighborhood of the endothelium.

Solution

Analytic solution. For first-order NO decomposition, the reaction-diffusion system, Eq. A2 with Eqs. A12 and A13 and Eqs. A14a and A15b, has an analytic solution. This solution is based on the general solution of Eq. A2, which is applied to each of the luminal, endothelial, and abluminal regions. For the luminal region

$$c_{\text{NO}} = C_1 I_0(\sqrt{k_{1,\text{NO}}} r) + C_2 K_0(\sqrt{k_{1,\text{NO}}} r) \quad (A17)$$

where I_0 and K_0 are the zero-order modified Bessel functions of the first and second kind, respectively, and the constants C_1 and C_2 are to be determined for the boundary conditions. A similar expression applies to each region, except the constants for the endothelium are C_3 and C_4 and the constants are C_5 and C_6 for the abluminal region. The boundary conditions (Eqs. A12 and A13) are automatically satisfied by requiring the concentration to remain finite at $r = 0$ and $r \rightarrow \infty$. This fixes C_1 and C_6 at 0, since $K_0(r) \rightarrow \infty$ as $r \rightarrow 0$ and $I_0(r) \rightarrow \infty$ as $r \rightarrow \infty$. The remaining constants are obtained by substituting the three equations for c_{NO} into the four boundary conditions (Eqs. A14 and A15). Solving the resulting system yields the four unknown constants.

The complete form of the analytic solution is not presented here because of its length, but it can be obtained from the authors on request. This analytic solution was used to verify

the numerical solution, which was used for most of the computations.

Numerical solution. The diffusion equation (Eq. A2) can be solved by several different numerical techniques. For the work here, we solved the non-steady-state form of Eq. A2

$$\frac{\partial c_{\text{NO}}^*}{\partial t^*} = \frac{1}{r^*} \frac{\partial}{\partial r^*} \left(r^* \frac{\partial c_{\text{NO}}^*}{\partial r^*} \right) - k^* c_{\text{NO}}^* \quad (A18)$$

Equation A18 was solved numerically and integrated up in time to steady state, $\partial c_{\text{NO}}^*/\partial t = 0$. This method has the advantage that transient behavior can be examined. Alternately, Eq. A2 could be discretized in r and solved by a finite-difference technique, or a shooting method could be used.

To solve Eq. A18, the partial differential equation was transformed to a system of ordinary differential equations in time by discretizing the spatial derivative (e.g., Eq. A3). We used second-order centered differencing, because its implementation is straightforward. The derivatives in the flux boundary conditions at the cell surfaces were discretized using forward or backward second-order accurate differencing. Because the concentration in the endothelium and close vicinity was of primary interest, variable grid spacing was used. This allowed the points near the endothelial surfaces, where the concentration gradients are steep, to be more closely spaced.

As is common for systems derived from parabolic partial differential equations, the system of ordinary differential equations was stiff. Our solution used the routines “odeint,” “stiff,” and “bstif” (3A); the routines “stiff” and “bstif” were modified to take advantage of the tridiagonal structure of the Jacobian matrix. We typically used a grid with 100–200 points. A finer grid does not materially change the result. With an error criterion for “stiff” of 3×10^{-4} and a grid of 100 points, the maximum difference between the computed solution and the analytic solution was $<5\%$. Although the boundary condition (Eq. A13) applies to an infinite domain, we solved them over a finite grid by applying Eq. A13 to the outermost points, typically 2,000–4,000 μm from the vessel axis. Several maximum distances were used to ensure that the result did not vary appreciably with the distance where the boundary condition was applied.

Sensitivity to parameters. In RESULTS we show the effect of luminal reaction rate and vessel diameter. Here, the sensitivity of the NO concentration to additional parameters is discussed. This effect is quantified by the sensitivity coefficient S defined by

$$S_i = \frac{p_i}{c_{\text{NO}}} \frac{\partial c_{\text{NO}}}{\partial p_i} \quad (A19)$$

where c_{NO} is evaluated at the abluminal endothelium interface and p_i is parameter i . The sensitivity coefficients were obtained from the analytic solution of the first-order reaction discussed above.

NO concentration was most sensitive to \dot{q}_{NO} for which $S_{\dot{q}_{\text{NO}}} = 1.0$. This is expected, since the boundary condition is linear in \dot{q}_{NO} .

We have assumed that the NO production rate does not vary with time and that the NO production was equally distributed between the abluminal and luminal surface of the endothelium; $f = 0.5$, where f is the fraction of total NO production from the abluminal surface of the endothelium

$$f = \dot{q}_{\text{NO,ab}} / (\dot{q}_{\text{NO,lu}} + \dot{q}_{\text{NO,ab}}) \quad (A20)$$

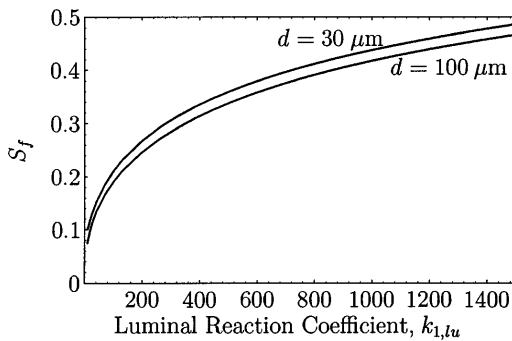


Fig. 5. Sensitivity coefficient (S_f) as a function of $k_{1,lu}$ for distribution of NO production between luminal and abluminal sides of endothelium. Parameter f is fraction of total NO produced from abluminal surface of endothelium. S_f is shown for 30- and 100- μm -diameter (d) vessels with $f = 0.5$, $k_{1,ab} = 0.01 \text{ s}^{-1}$, and $\dot{q}_{\text{NO}} = 5.3 \times 10^{-14} \mu\text{mol} \cdot \mu\text{m}^{-2} \cdot \text{s}^{-1}$.

To investigate the effect of this parameter, we define the sensitivity coefficient

$$S_f = \frac{f}{c_{\text{NO}}} \frac{\partial c_{\text{NO}}}{\partial f} \quad (\text{A21})$$

The NO concentration can be strongly affected by this distribution (Fig. 5). Although S_f is essentially independent of vessel diameter, it does depend on $k_{1,lu}$. This is because the endothelium provides resistance to mass transfer, so NO produced on the abluminal side is "protected" from scavenging by the blood. As $k_{1,lu}$ decreases, less NO is scavenged by the blood, so the effect diminishes.

We also assumed that the luminal and abluminal diffusion coefficients were the same. The effect of the luminal diffusion coefficient can be characterized by

$$S_{D_{lu}} = \frac{D_{lu}}{c_{\text{NO}}} \frac{\partial c_{\text{NO}}}{\partial D_{lu}} \quad (\text{A22})$$

The dependence of endothelial NO concentration on $S_{D_{lu}}$ is appreciable (Fig. 6). Because $S_{D_{lu}}$ is negative, decreasing D_{lu} increases the NO concentration. This effect is opposite of what might be expected (see *Boundary conditions*), and it is caused by the reduction of the concentration gradient near the vessel wall. As $k_{1,NO}$ decreases, $S_{D_{lu}}$ becomes dependent on the vessel size, with less effect in the smaller vessels. This is because the NO concentration gradient is less steep for small vessels than for large vessels.

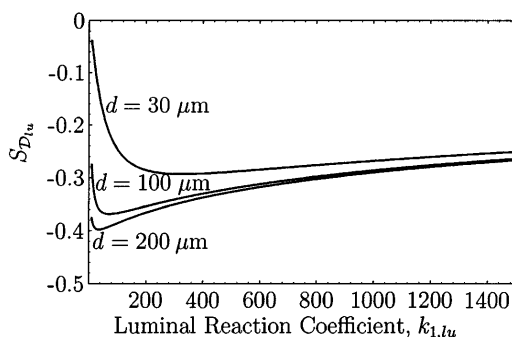


Fig. 6. Sensitivity coefficient ($S_{D_{lu}}$) as a function of $k_{1,lu}$ for luminal diffusion coefficient (D_{lu}) for 30-, 100-, and 200- μm -diameter vessels and $k_{1,ab} = 0.01 \text{ s}^{-1}$ and $\dot{q}_{\text{NO}} = 5.3 \times 10^{-14} \mu\text{mol} \cdot \mu\text{m}^{-2} \cdot \text{s}^{-1}$.

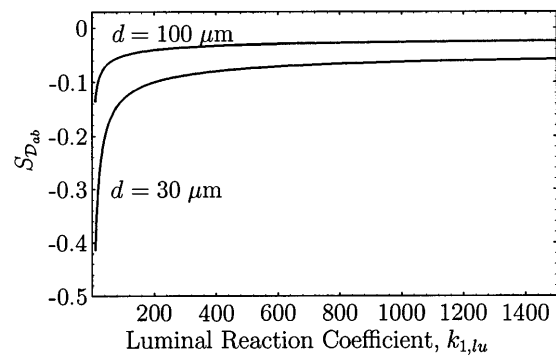


Fig. 7. Sensitivity coefficient ($S_{D_{ab}}$) as a function of $k_{1,lu}$ for luminal diffusion coefficient (D_{ab}) for 30- and 100- μm -diameter vessels and $k_{1,ab} = 0.01 \text{ s}^{-1}$ and $\dot{q}_{\text{NO}} = 5.3 \times 10^{-14} \mu\text{mol} \cdot \mu\text{m}^{-2} \cdot \text{s}^{-1}$.

The sensitivity of the endothelial NO concentration to the abluminal diffusion coefficient (D_{ab})

$$S_{D_{ab}} = \frac{D_{ab}}{c_{\text{NO}}} \frac{\partial c_{\text{NO}}}{\partial D_{ab}} \quad (\text{A23})$$

is seen in Fig. 7. The effect is appreciable only if the luminal reaction rate $k_{1,lu}$ is low and the vessel is small. This indicates that D_{ab} influences the endothelial NO concentration most if NO degradation in the lumen is relatively low, so the flux of NO into the abluminal region is substantial.

This work was sponsored by a Whitaker Foundation Biomedical Engineering Research Grant and National Science Foundation Grant BES-9511737.

Address for reprint requests: J. C. Liao, Dept. of Chemical Engineering, University of California, Los Angeles, CA 90095-1592.

Received 12 September 1997; accepted in final form 7 January 1998.

REFERENCES

1. **Albina, J. E., and R. B. Mateo.** Nitric oxide. In: *Amino Acid Metabolism and Therapy in Health and Nutritional Disease*. Boca Raton, FL: CRC, 1995, p. 99–123.
2. **Baez, S.** Simultaneous measurements of radii and wall thickness of microvessels in the anesthetized rat. *Circ. Res.* 25: 315–329, 1969.
3. **Bassingthwaight, J. B., C. Y. Wang, and I. S. Chan.** Blood-tissue exchange via transport and transformation by capillary endothelial cells. *Circ. Res.* 65: 997–1020, 1989.
4. **Baxter, L. T., and R. K. Jain.** Transport of fluid and macromolecules in tumors. IV. A microscopic model of the perivascular distribution. *Microvasc. Res.* 41: 252–272, 1991.
5. **Carlsen, E., and J. H. Comroe, Jr.** The rate of uptake of carbon monoxide and of nitric oxide by normal human erythrocytes and experimentally produced spherocytes. *J. Gen. Physiol.* 42: 83–107, 1958.
6. **Cassoly, R., and Q. Gibson.** Conformation, co-operativity and ligand binding in human hemoglobin. *J. Mol. Biol.* 91: 301–313, 1975.
7. **Chien, S., S. Usami, and R. Skalak.** Blood flow in small tubes. In: *Handbook of Physiology. The Cardiovascular System. Microcirculation*. Bethesda, MD: Am. Physiol. Soc., 1984, sect. 2, vol. IV, pt. 1, chapt. 6, p. 217–249.
8. **Duling, B. R., W. Kuschinsky, and M. Wahl.** Measurements of the perivascular Po_2 in the vicinity of the pial vessels of the cat. *Pflügers Arch.* 383: 29–34, 1979.
9. **Eich, R. E., T. Li, D. D. Lemon, D. H. Hoherty, S. N. Curry, A. J. Matthews, K. A. Johnson, R. D. Smith, G. N. Phillips, Jr., and J. S. Olson.** Mechanism of NO-induced oxidation of myoglobin and hemoglobin. *Biochemistry* 35: 6976–6983, 1996.
10. **Ekelund, U., and S. Mellander.** Role of endothelium-derived nitric oxide in the regulation of tonus in large-bore arterial

- resistance vessels, arterioles and veins in cat skeletal muscle. *Acta Physiol. Scand.* 140: 301–309, 1990.
11. **Falcone, J. C., and H. G. Bohlen.** EDRF from rat intestine and skeletal muscle venules causes dilation of arterioles. *Am. J. Physiol.* 258 (*Heart Circ. Physiol.* 27): H1515–H1523, 1990.
 12. **Fischkoff, S., and J. M. Vanderkooi.** Oxygen diffusion in biological and artificial membranes determined by the fluorochrome pyrene. *J. Gen. Physiol.* 65: 663–676, 1975.
 13. **Fung, Y. C.** *Biomechanics: Motion, Flow, Stress, and Growth.* New York: Springer-Verlag, 1990.
 14. **Garg, U. C., and A. Hassid.** Nitric oxide generating vasodilators and 8-bromo-cyclic guanosine monophosphate inhibit mitogenesis and proliferation of cultured rat vascular smooth muscle cells. *J. Clin. Invest.* 88: 4651–4655, 1989.
 15. **Hess, J. R., V. W. MacDonald, C. S. Gomez, and V. Coppers.** Increased vascular resistance with hemoglobin-based oxygen carriers. *Artif. Cells Blood Substit. Immobil. Biotechnol.* 22: 361–372, 1994.
 16. **Ignarro, L. J.** Biosynthesis and metabolism of endothelium-derived nitric oxide. *Annu. Rev. Pharmacol. Toxicol.* 30: 535–560, 1990.
 17. **Jia, L., C. Bonaventura, J. Bonaventura, and J. S. Stamler.** S-nitrosohaemoglobin: a dynamic activity of blood involved in vascular control. *Nature* 380: 221–226, 1996.
 18. **Kubes, P., M. Suzuki, and D. N. Granger.** Nitric oxide: an endogenous modulator of leukocyte adhesion. *Proc. Natl. Acad. Sci. USA* 88: 4651–4655, 1991.
 19. **Kuo, L., W. M. Chilian, and M. J. Davis.** Coronary arteriolar myogenic response is independent of endothelium. *Circ. Res.* 66: 860–866, 1990.
 20. **Kuo, L., M. J. Davis, and W. M. Chilian.** Longitudinal gradients for endothelium-dependent and -independent vascular responses in the coronary microcirculation. *Circulation* 92: 518–525, 1995.
 21. **Lancaster, J. R.** Simulation of the diffusion and reaction of endogenously produced nitric oxide. *Proc. Natl. Acad. Sci. USA* 91: 8137–8141, 1994.
 22. **Lancaster, J. R.** Diffusion of free nitric oxide. *Methods Enzymol.* 268: 31–50, 1996.
 23. **Lancaster, J. R.** A tutorial on the diffusivity and reactivity of free nitric oxide. *Nitric Oxide* 1: 18–30, 1997.
 24. **Laurent, M., M. Lepoivre, and J.-P. Tenu.** Kinetic modelling of the nitric oxide gradient generated in vitro by adherent cells expressing inducible nitric oxide synthase. *Biochem. J.* 314: 109–113, 1996.
 25. **Liao, J. C., and L. Kuo.** Interaction between adenosine and flow-induced dilation in coronary microvascular network. *Am. J. Physiol.* 272 (*Heart Circ. Physiol.* 41): H1571–H1581, 1997.
 26. **Lightfoot, E. N.** *Transport Phenomena and Living Systems.* New York: Wiley, 1974.
 27. **Lloyd-Jones, D. M., and K. D. Bloch.** The vascular biology of nitric oxide and its role in atherogenesis. *Annu. Rev. Med.* 47: 365–375, 1996.
 28. **Malinski, T., Z. Taha, S. Grunfeld, S. Patton, M. Kapturczak, and P. Tomboulian.** Diffusion of nitric oxide in the aorta wall monitored in situ by porphyrinic microsensors. *Biochem. Biophys. Res. Commun.* 193: 1076–1082, 1993.
 29. **McGill, H. C.** *The Geographic Pathology of Atherosclerosis.* Baltimore, MD: Williams & Wilkins, 1968, p. 1–193.
 30. **Moncada, S., and A. Higgs.** The L-arginine-nitric oxide pathway. *N. Engl. J. Med.* 329: 2002–2012, 1993.
 31. **Moncada, S., and A. Higgs.** Molecular mechanisms and therapeutic strategies related to nitric oxide. *FASEB J.* 9: 1319–1330, 1995.
 32. **Moncada, S., M. J. Palmer, and E. A. Higgs.** Nitric oxide: physiology, pathophysiology, and pharmacology. *Pharmacol. Rev.* 43: 109–142, 1991.
 33. **Pitman, R. N.** Influence of microvascular architecture on oxygen exchange in skeletal muscle. *Microcirculation* 2: 1–18, 1995.
 34. **Pohl, U., and D. Lamontagne.** Impaired tissue perfusion after inhibition of endothelium-derived nitric oxide. *Basic Res. Cardiol.* 86, Suppl. 2: 97–105, 1991.
 35. **Popel, A. S.** Theory of oxygen transport to tissue. *Crit. Rev. Biomed. Eng.* 17: 257–321, 1989.
 36. **Radomski, M. W., R. M. J. Palmer, and S. Moncada.** An L-arginine/nitric oxide pathway present in human platelets regulates aggregation. *Proc. Natl. Acad. Sci. USA* 87: 5193–5197, 1990.
 37. **Saito, Y., A. Eraslan, V. Lockard, and R. L. Hester.** Role of venule endothelium in control of arteriolar diameter during functional hyperemia. *Am. J. Physiol.* 267 (*Heart Circ. Physiol.* 36): H1227–H1231, 1994.
 38. **Schmidt-Schönbein, H., T. Fisher, G. Driessen, and H. Rieger.** *Microcirculation.* Baltimore, MD: University Park, 1979, p. 353–418.
 39. **Shimokawa, H., and A. Takeshita.** Endothelium-dependent regulation of the cardiovascular system. *Intern. Med.* 34: 939–946, 1995.
 40. **Stamler, J. S., O. Jaraki, J. Osborne, D. I. Simon, J. Keaney, J. Vita, D. J. Singel, C. R. Valeri, and J. Loscalzo.** Nitric oxide circulates in mammalian plasma primarily as an S-nitroso adduct of serum albumin. *Proc. Natl. Acad. Sci. USA* 89: 7674–7677, 1992.
 41. **Stone, J. R., and M. A. Marletta.** Spectral and kinetic studies on the activation of soluble guanylate cyclase by nitric oxide. *Biochemistry* 35: 1093–1099, 1996.
 42. **Vaughn, M. W., L. Kuo, and J. C. Liao.** Estimation of nitric oxide production and reaction rates in tissue using a mathematical model. *Am. J. Physiol.* In press.
 43. **Wood, J., and J. Garthwaite.** Models of the diffusional spread of nitric oxide: implications for neural nitric oxide signalling and its pharmacological properties. *Neuropharmacology* 33: 1235–1244, 1994.
 44. **Zuck, T. F., and J. G. Riess.** Current status of injectable oxygen carriers. *Crit. Rev. Clin. Lab. Sci.* 31: 295–324, 1994.
 - 1A. **Finlayson, B. A.** *Nonlinear Analysis in Chemical Engineering.* New York: McGraw-Hill, 1980, p. 214.
 - 2A. **Malinski, T., Z. Taha, S. Grunfeld, S. Patton, M. Kapturczak, and P. Tomboulian.** Diffusion of nitric oxide in the aorta wall monitored in situ by porphyrinic microsensors. *Biochem. Biophys. Res. Commun.* 193: 1076–1082, 1993.
 - 3A. **Press, W. H., B. P. Flannery, S. A. Teukolsky, and W. T. Vetterling.** *Numerical Recipes in C* (2nd ed.). Cambridge, UK: Cambridge University Press, 1992.
 - 4A. **Slattery, J. C.** *Momentum, Energy, and Mass Transfer in Continua* (2nd ed.). Malabar, FL: Kreiger, 1981, p. 482, 451.